

Oscillations Damping Enhancement using Load Frequency Control and Improved Power System Stabilizer Considering Wind Power Integration

Nesrine MEKKI^{1*}, Lotfi KRICHEN^{1a}

¹Department of Electrical Engineering, ENIS, Tunisia

*Corresponding author, Doctor-Engineer, E-mail: mekki_nesrine@hotmail.fr

^aProfessor, E-mail: lotfi.krichen@enis.tn

Abstract. *The undamped oscillations problem in an interconnected power system has been a matter of concern in several power systems for a long time. In fact, the oscillatory response of power plants under normal and fault conditions is one of the most dominant grid connection requirements to be met by robust control systems. This paper presents a new control scheme coordinating the Load Frequency Control (LFC) process with an Improved Power System Stabilizer (IPSS) loop whose main purpose is the power swings damping enhancement whenever subjected to sudden changes in load levels as well as disturbances. Accordingly, a performant tuned PI controller for LFC and an IPSS tuning method, are thoroughly discussed. Additionally, the impact of integrated wind farms of Doubly-Fed Induction Generator (DFIG) on the studied power system stability is investigated under different operating conditions. The simulation results of a modified 9-Bus IEEE test system are carried out proving the proposal's applicability.*

Keywords: *Load Frequency Control, Optimal Tuning, Improved Power System Stabilizer, PI Controller, Doubly-Fed Induction Generator*

1. INTRODUCTION

Recently, with the rapid increase in energy demand, operation and control of interconnected power systems become one of the challenging issues to ensure sustainable and reliable supply. Practically, unpredictable load deviations even with slight amount may affect the nominal system behavior regarding especially its frequency value and the scheduled power exchanges [1]. Thus, modern energy management systems implicate several multi-level control schemes for each area such as importantly the Automatic Generation Control (AGC), commonly referred to load-frequency control (LFC), which constitutes almost additional secondary control aiming to eliminate the system deviations [2]. This control has been implemented adding an Area Control Error (ACE), which acts on the Turbine Governor's (TG) load reference settings [3]. It is a function of the real power interchange variations that the AGC mechanism desires to make zero [4] [5]. Literately,

for a multi area system, various generation control strategies have been proposed since the 1970s [2] [6]. In fact, in [7], an overview about the AGC issue has been reported, it includes an overview of its schemes, power system models, control techniques, load characteristics, and its coordination with the renewable resources.

Likewise, a review of LFC's control design has been revealed different approaches generally related to Proportional–Integral–Derivative (PID), full state feedback, adaptive and variable structure, intelligent, and networked control schemes. Pandey et al. suggested a thorough survey of LFC issue for distribution and conventional power systems [8]. Rerkpreedapong et al. proposed two robust decentralized control designs [9] using linear matrix inequalities technique and Proportional-Integral (PI) basically tuned by the genetic algorithm. Similarly, Yu et al. presented a linear matrix inequalities based robust controller taking into consideration the communication delays [10]. The fuzzy controller is investigated in [11]. In [12], the sliding mode controller is recommended. Particularly, among all these proposals, PI controllers are frequently adopted in industrial applications in order to reduce the steady-state error to zero [13]. Previous studies have presented a combined LFC-AVR control design for power system stability improvements. In fact, the main concern was to judge only the mutual effects between LFC and AVR loops by coordinating a redesigned PSS [14]. In [15], the artificial bee colony approach has been applied. Other investigations using the metaheuristic bat inspired algorithm have been proposed in order to improve the LFC and AVR control strategies [16].

As a matter of fact, monitoring modern interconnected power systems effectively may necessitate the involvement of auxiliary powerful regulators such as the Power System Stabilizer (PSS) that aims basically to resolve oscillatory stability troubles as well as they are technically ameliorated. Over the last few decades, the great growth in electrical links were hosted new kinds of oscillation between the different areas constituting the power system. In fact, in case of large

immersion, inter-area modes possibly will be as low as 0.2 Hz. Besides, inter-machines oscillations in certain power plant could attain frequencies as high as 4.0 Hz with small machine inertia and high exciter gains [17]. Hence, damping all these oscillating modes efficiently is the major task that a PSS must assign. Literately, PSSs that are out of service or poorly tuned are the major stimulators of several blackouts such as the western U.S. in 1996. Additionally, even these difficulties have been fixed, great disturbances tend to induce 0.2Hz low-frequency oscillations in the network [18]. In point of fact, in Brazil for example, the north-south interconnection has witnessed an increase to a new low-frequency inter-area mode needing a retuning of the existing PSSs [18]. Meanwhile, by retuning and coordinating PSSs efficiently, utilities are able enough to enhance extremely the damping of dominant inter-area modes. The most of the existing PSSs are power acceleration analog devices, but far ahead, modern manufacturers offer a digital PSS, denoted as PSS2B, which can be tuned simply as a speed-based PSS [19]. Later, a novel PSS design was suggested in [20] and incorporated in the revised IEEE standards as PSS4B. As well, it builds on a simple multiband transfer function while offering robust PSS tuning over a wide range of frequency. A thorough evaluation of these two types of PSSs was extensively explained in [18]. Likewise, recent researches focused on comparing different types of PSS taking into account its ability in judging local-mode and inter-area damping performances especially while facing the possible adverse factors.

The growing amount in electricity consumption stimulates the need to investigate the renewable energy resources. Chiefly, wind energy has witnessed a great revolution in several countries which try to carry out detailed analysis of its impact on their grid stability [21]. In fact, these studies deal mainly with different challenging aspects such as the fluctuating nature of wind power, its location, the generator technologies and its control strategy. The literature review has been presented various wind turbine generator technologies and has been focused basically on analyzing its influence and applicability in the power system under both disturbances and normal conditions. Generally, three types of wind turbine are widely used in industry namely, squirrel cage induction generator, direct drive synchronous generator, and especially Doubly Fed Induction Generator (DFIG) which becomes increasingly popular among the wind power conversion systems. Several comparative studies have been revealed the differences between these concepts regarding the

generating system and the rotor aerodynamic efficiency especially during high wind speeds [22].

The contribution of this paper is to investigate a new combination between an optimal LFC design and an Improved Power System Stabilizer (IPSS) in order to damp effectively power system oscillations and enhance the dynamic performances. The performed LFC design is basically equipped with a PI controller whose parameters are optimally tuned using a nonsmooth H_∞ optimization technique. Later, in order to reinforce the operational grid capabilities while damping its fluctuations, a modified Multi Band-Power System Stabilizer (MB-PSS) is added and favorably tuned in the control process using the symmetrical approach which helps to meet the increasing load demand requirements. The whole system then will be subjected to a disturbance to validate the role of the coordinated AGC-IPSS design in restoring the system balance. The rest of paper carries out the performance validation of the suggested controllers in a modified IEEE 9-bus test system including DFIG wind turbines under different operating conditions.

2. Proposed Control Strategy

The research under investigation concerning power system control suggested a coordinated AGC-IPSS design as a challenging issue helping in monitoring the upcoming advances while keeping reasonably uniform system frequency.

2.1. PI-Based LFC Design

The change in frequency occurs whenever the load changes randomly. The error signal is amplified, mixed and transmuted into real power command signal which is dispatched then to the TG rising the torque value. The governor operates to restore the balance between the input and output by changing the turbine output while respecting the specified tolerance [23].

Evidently, an auxiliary control action of a PI controller is chosen to be included in the present work as depicted in Fig. 1 in order to ensure a robust AGC loop design that keeps the power plant frequency under its nominal value. Fig. 2 displays the models of hydraulic turbine and governor associated with the synchronous machine block. Initially, the power system operates without wind power integration which will be the main purpose of the next section. All the system parameters are given in the Appendix.

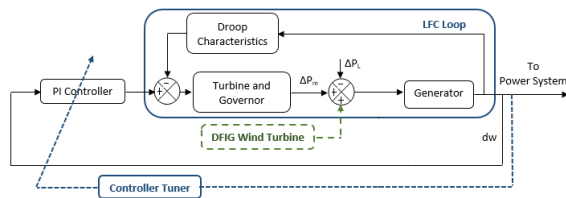


Fig. 1. Block diagram of AGC design in a single area power plant with DFIG

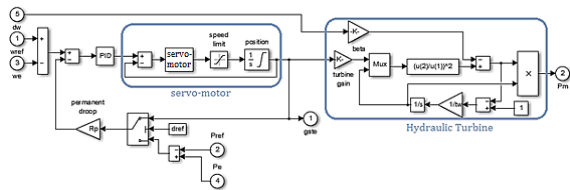


Fig. 2. Block diagram of hydraulic turbine and governor

- dw Speed deviation (Hz)
- ΔP_m Change in mechanical power (pu)
- ΔP_L Load disturbance (pu)

Compared to multiple candidate control techniques such as PID, intelligent control (hybrid neuro fuzzy and fuzzy logic controllers..), variable structure, full state feedback (linear quadratic regulator) and other advanced strategies, PI controllers still widely used in industries thanks to their simplicity. Yet, in order to assure high dynamic system performances, tuning a PI regulator parameters becomes critical especially to meet the system non-linearity and its high complexity requirements [24]. Almost, as the dynamics of the investigated power system are typically nonlinear, special attentions are considered for designing the PI controller as follows [25][26]:

Each area contributes to the frequency control and regulates its own load variations. Transient behavior should be reached optimally.

In steady state, frequency and tie-line power exchanges are, respectively, returned to their nominal values (ACE = 0).

The controller would be robust to meet the system parameters variation. As manual procedures are time-consuming, searching for new PI tuning software may help to meet the aims of tuning automatically the controller parameters while keeping a reasonable tradeoff between performance and robustness and offering simultaneously the desirable maximum overshoot, the phase and gain margins and the bandwidth of the closed-loop system. Therefore, the controller parameters are optimally selected through a PID tuner which provides a fast applicable single-loop tuning method with transfer function based-settings.

PI parameters can be easily tuned while reaching a robust design with the desired response time. First, the software computes a linearized plant model perceived by the controller, identifies its input and output automatically, and uses the actual operating point for the linearization.

The tuning approach deals mainly with the non-smooth H_∞ minimization technique. It solves the following constrained problem:

$$\text{Minimize } \max_i f_i(x) \quad (1)$$

- $f_i(x)$ and $g_j(x)$ are the normalized values of soft and hard tuning requirements [24].

Subject to (2)

- $\max_j g_j(x) < 1$, for $x_{\min} < x < x_{\max}$
- x is the vector of PI parameters to tune.
- x_{\min} and x_{\max} are the minimum and maximum values of the free parameters of the controller.

In point of view of the tuning goals [27], the software approaches the optimization problem by resolving a sequence of unconstrained subproblems given by:

$$\min_x \max(\alpha f(x), g(x)) \quad (3)$$

The multiplier ' α ' is adjusted so that the solution converges to the solution of the original constrained optimization problem. Afterward, the tuning process will give new values of PI parameters that best solve the minimization problem. The block performances are verified finally in the test system.

Additionally, in order to identify the optimal tuning method, a comparison study of using different optimization techniques may be significantly important. Thus, three criterions such as the Integral of the Square of the Error (ISE), Integral of the Absolute value of Error (IAE) and Integral of Time-weighted Absolute Error (ITAE) are calculated for each algorithm to evaluate the controller response. Meanwhile, the main objective here is to obtain the minimum values of these performance indices which are defined as follows:

$$ISE = \int_0^\infty ACE^2 dt$$

$$IAE = \int_0^\infty |ACE| dt$$

$$ITAE = \int_0^\infty |ACE| t dt$$

Literately, the ITAE minimization is mostly referred as a good tuning criterion to get PI parameters and useful index which penalizes long-duration transients. The system response could have then a settling time much more quickly using the ITAE than using the ISE which penalizes in general large errors more than smaller ones. Likewise, to eliminate small errors, IAE index is accordingly taken into account as it affords slower

response than ISE with less sustained fluctuations [28]. Hence, a great attention will be given importantly to the IAE and ITAE indices which help later to compare different tuning methods.

2.2. Investigated IPSS Design

Referring to several comparative studies, The IPSS model on which investigations in this paper are carried out is mainly based on the MB-PSS model (IEEE PSS4B) which presents competitive features in comparison with other controllers. Actually, it keeps greatly most of the PSS2B properties in local and torsional modes using an electrical power transducer that tracks high-frequency dynamics as well as affording an improved lower-frequency inter-area modes. Fig. 3 depicts the additional control loop of the performed IPSS which is installed in the excitation system whose block diagram is presented in Fig. 4.

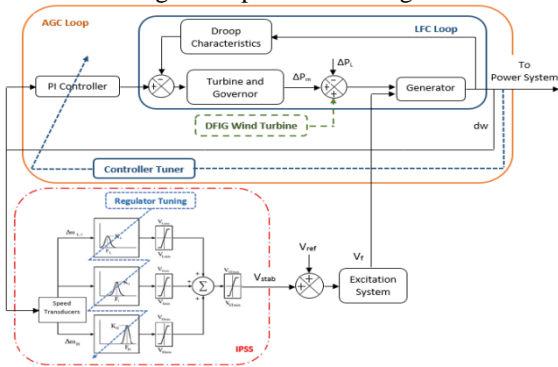


Fig. 3. Block diagram of the coordinated LFC-IPSS design in a single area power plant

- V_{ref} Reference voltage (pu)
- V_f Field voltage (pu)
- F_L Center frequency of low frequency band
- K_L Peak gain of the low frequency band
- F_I Center frequency of the intermediate frequency band
- K_I Peak gain of the intermediate frequency band
- F_H Center frequency of the high frequency band
- K_H Peak gain of the high frequency band
- V_{Smax} Limits imposed on the output of the stabilizer.
- V_{stab} Stabilization voltage (pu)

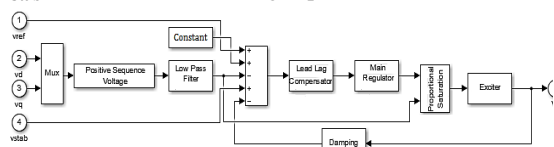


Fig. 4. Block diagram of the excitation system associated to the generator

The MB-PSS block diagram constituting the

IPSS block comprises principally three functions, namely the transducers, the lead-lag compensation and the limiters. In fact, two speed deviation transducers are implemented in the structure to feed three bands defining the lead-lag compensation. In addition to that, four adaptable limiters are offered for each band and the whole PSS output.

In fact, the low band concerns very slow oscillating phenomena like common modes possibly created on isolated systems with frequency range typically under 0.2 Hz. The intermediate band deals with inter-area modes often found in the range of 0.2 to 1.0 Hz while the high band concerns local modes, either plant or inter-machines, with a frequency range of 0.8 to 4.0 Hz. Besides, the speed deviation transducers are linked with the machine terminal currents and voltages. The first one measures accurately in the 0 to 2.0 Hz range, while the second one is intended for the high band with a range of frequency of 0.8 to 5.0 Hz. Importantly, the lead-lag compensation circuit is globally identified with six parameters which are the three filter central frequencies F_L, F_I, F_H and the gains K_L, K_I, K_H . They are primarily required for efficient IPSS tuning. Time constants and branch gains for the low band case satisfy the following equations [29]:

$$T_{Li} = \frac{1}{2\pi F_L \sqrt{R}} \quad \text{for } i=2,7 \quad (7)$$

$$T_{L1} = \frac{T_{L2}}{R} \quad (8)$$

$$T_{L8} = T_{L7} \cdot R \quad (9)$$

$$K_{Li} = \frac{R^2 + R}{R^2 - 2R + 1} \quad \text{for } i=1,2 \quad (10)$$

Table 1 proposes four candidate settings for the PSS4B [29]. They were elected from recent researches closely reflecting the greatest practices in the tuning process.

The strategy of the current study deals mainly with the symmetrical approach which is based on varying the center frequency and gain of each band so as to accomplish a nearly flat phase response at the frequency of interest which is globally between 0.1 Hz and 5Hz.

Table 1. Proposed Settings for PSS4B

| Settings | 1 | 2 | 3 | 4 | 5 |
|---|-------|-------|-------|-------|-------|
| $R=1.2, V_{smax} = -V_{smin} = 0.1$ | | | | | |
| $V_{lmax} = -V_{lmin} = V_{hmax} = -V_{hmin} = 0.6$ | | | | | |
| V_{Lmin} | -0.04 | -0.04 | -0.04 | -0.02 | -0.02 |
| V_{Lmax} | +0.08 | +0.08 | +0.08 | +0.02 | +0.02 |
| K_L | 20.5 | 13.7 | 13.7 | 6 | 6 |
| F_L | 0.116 | 0.116 | 0.116 | 0.08 | 0.19 |
| K_I | 41 | 27.3 | 31 | 27 | 30 |
| F_I | 0.506 | 0.506 | 0.506 | 0.8 | 1.1 |
| K_H | 85 | 75 | 68 | 159 | 150 |
| F_H | 12.1 | 12.1 | 12.1 | 12.1 | 12 |

Setting 1 is the base core from which further sets are derived. Even it reaches relatively a uniform phase advance, this kind of PSS can support high gain whenever needed. The second setting helps in decreasing low-, intermediate-, and high-frequency gains. Setting 3, approximately same as setting 2, adds a washout in the high-frequency band in order to reduce the sensitivity to fast mechanical power ramps. Besides, setting 4 is the simple tuning one. It is based on three symmetrical bands related mainly to six parameters and designated to mimic setting 2 over a wide range of frequency.

Accordingly, based on the selected set, the IPSS parameters are tuned and mentioned as ‘Setting 5’ which diminishes fruitfully the regulator complexity without losing out so much on performance. In fact, this setting reveals the greatest oscillations damping as depicted in Fig. 5 which presents the frequency response of ‘Gen 2’ for different MB-PSS settings. As well, comparison between simulations shows the difference in frequency between all the settings as displayed in Fig. 6.

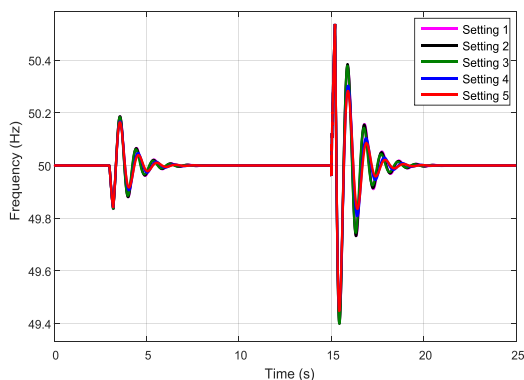


Fig. 5. Frequency response of ‘Gen 2’ for different settings under fault conditions

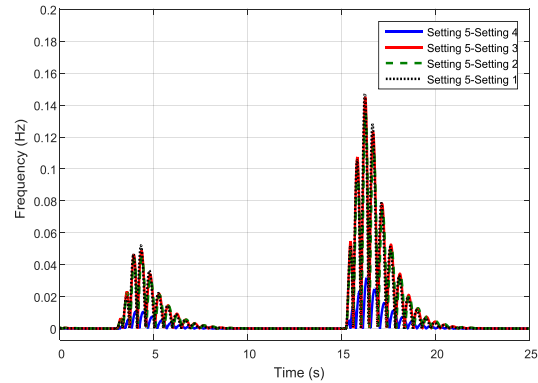


Fig. 6. Difference in frequency between the proposed settings

3. DFIG Wind Turbines Integration

The simulation study of the investigated test system including DFIG wind turbines as shown in Fig. 1 aims essentially to highlight the impact of renewable energy whenever integrated on the power system under normal conditions as well as under disturbance. Meanwhile, treating the dynamic performances of this kind of turbines becomes a challenging issue that may affect the system stability. Reciprocally, this technology is able enough to support the grid with the appropriate reactive power and stable frequency and voltage, as well as helping in damping the power oscillations [30-32].

The impact of wind power generation on the dynamic behavior of network is a key factor in considering a robust LFC design which may improve the system frequency response whenever exposed to slow changes of load and renewable resource especially in case of a disturbance event as it attracts more reactive power which may lead to withering voltage drop.

Commonly, conventional power plants are rather effective at adjusting the power output to meet the load balance. Still, due to wind power intermittency, it is more difficult for wind turbines to track the load demand variation. Therefore, simulation purposes address mainly the robustness of the optimized LFC loop in coordination with the performed IPSS while restraining the frequency deviation efficiently and showing faster response and stability.

4. Simulation and Results

The IEEE 9-bus system illustrated in Fig. 7 is adopted in this study. This test case represents a simple approximation of the western system coordinating council to an equivalent system with 9 buses, 3 generators, 3 two-winding power transformers, 6 lines and 3 loads. The line

complex powers are around hundreds of MVA each and the voltage levels are 13.8 kV, 16.5 kV, 18 kV, and 230 kV. ‘Gen 1’ designs the swing generator. The standard test system witnessed a modification regarding the generators ‘Gen 2’ and ‘Gen 3’ which are replaced by new power plants involving similarly the LFC and IPSS equipments as well as integrating DFIG wind turbines in an advanced step. The proposed control scheme is incorporated into the HTG and excitation system blocks as shown in Fig. 8.

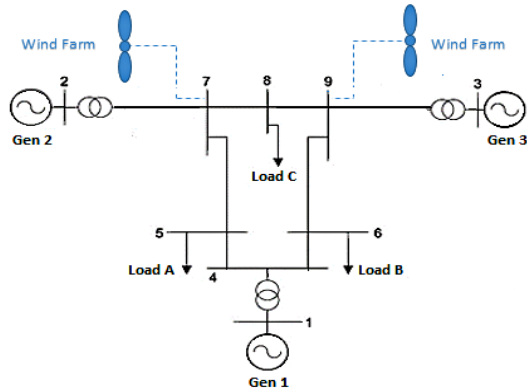


Fig. 7. 9-Bus IEEE test system

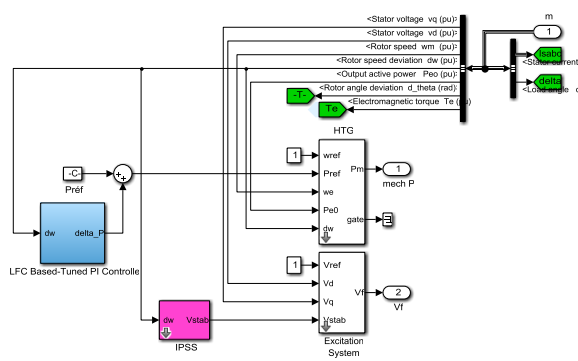


Fig. 8. Simulink model of the Hydraulic Turbine and Governor (HTG) and Excitation System blocks associated to Generator ‘Gen 2’

4.1. LFC Based-Tuned PI Controller Impact

The major interest is to evaluate first the designed LFC performances in an interconnected power system basically related to the loading conditions.

According to Fig. 9 which depict the frequency response delivered by ‘Gen 2’, it’s clear that after its integration, the swings constituting the signal decrease in number and amplitude to get finally a frequency recovered close to the nominal frequency which is around 50 Hz. Particularly, the sudden increase in load demand at 3 s causes thorough frequency perturbations which are attenuated gradually. Meanwhile, AGC application may help significantly in maintaining the frequency

at the scheduled values.

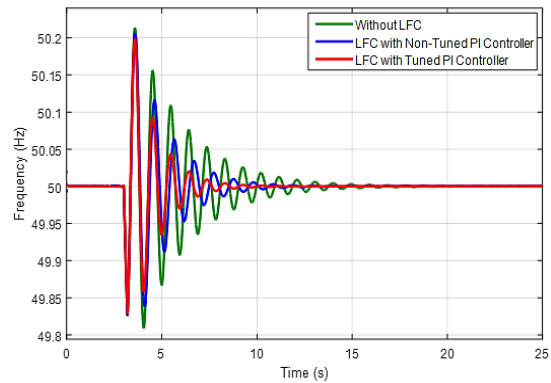


Fig. 9. Frequency Response of Generator ‘Gen 2’

In fact, choosing randomly the controller parameters may not ensure the best performances regarding the frequency’s stability. Yet, the application of the tuning process reveals better frequency response nearly close to the nominal system frequency. Actually, during overloading condition, the frequency deviations persist for a long period, thus, with the optimized LFC loop, the governor system will be able to absorb effectively the frequency fluctuations. Simulation results prove definitely that LFC based-tuned PI controller application can damp efficiently the frequency oscillations in reaction to the changing demand. Beforehand, In order to justify the efficiency of the proposed method, several approaches are implemented and applied for optimal tuning of PI parameters. In fact, based on the comparative analysis shown in Table 2, the non-smooth optimization technique is chosen to be adopted in this study as it demonstrates its excellence in giving better results by affording the least values of IAE and ITAE indices and meeting the desired requirements.

Table 2. Comparison of Performance Indices for PI controller

| Tuning Approach Performance Indices | Genetic Algorithm | Simpl ex Search | Sequential Quadratic Programming | Active Set | Nonsmooth H _∞ |
|-------------------------------------|--------------------------|--------------------------|----------------------------------|--------------------------|--------------------------|
| ISE | 7.26 10 ⁻⁵ | 7.22 10 ⁻⁵ | 7.32 10 ⁻⁵ | 7.29 10 ⁻⁵ | 7.29 10 ⁻⁵ |
| IAE | 0.015 | 0.016 | 0.016 | 0.015 | 0.015 |
| ITAE | 0.24 | 0.24 | 0.24 | 0.24 | 0.23 |

Eventually, as the system voltage and frequency responses are strongly sensitive even to slight changes in load, results will take into account the effect of the designed LFC connection particularly on the load buses. Therefore, analysis will basically

focus on the nearest variable load located at bus 8. Its voltage magnitude profile is shown in Fig. 10.

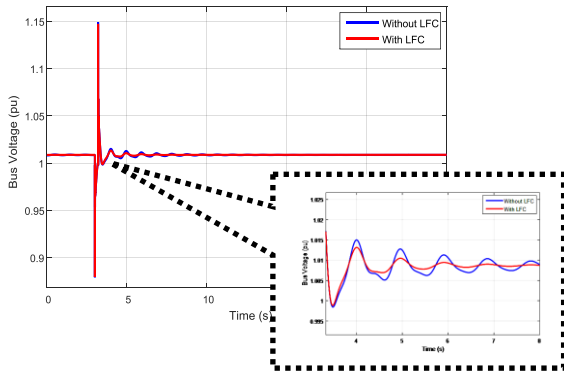


Fig. 10. Voltage Profile of Bus 8

Evidently, it is clearly shown that the load variation would cause remarkable perturbations which are later damped out significantly after integrating the performed LFC process into the system.

4.2. Involvement of IPSS Control

In addition to the performed LFC equipment, the designed IPSS is now installed for each generator. Its parameters are tuned and defined in ‘setting 5’ as mentioned previously in Table 1. The IPSS frequency response is definitely plotted in Fig. 11.

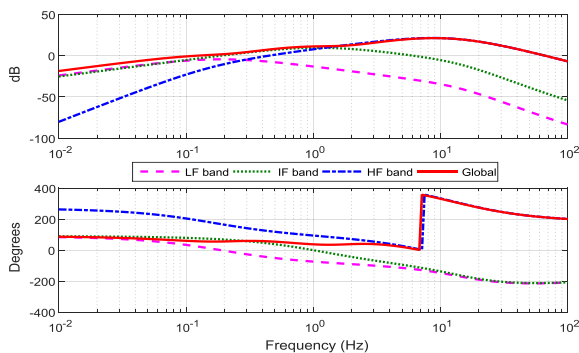


Fig. 11. IPSS Frequency Response

Evidently, the IPSS gains seem to be more aggressive and consequently more effective especially in the critical inter-area frequency range from 0.1 to 1 Hz. Furthermore, its frequency response confirms definitely that the IPSS phase is nearly flat around 80 degrees in the frequency range of interest. In fact, to guarantee robust damping, this PSS ought to imply, at all frequencies of interest, a moderate phase advance in order to compensate the lag created between the field excitation and the electrical torque.

For reasons of simplicity, this study chooses as example of concern the generator number 2 ‘Gen 2’. IPSS will definitely control the excitation

system in order to reduce the power swings rapidly as shown in Fig. 12 which depicts the frequency response of ‘Gen 2’ in reaction to the load variation.

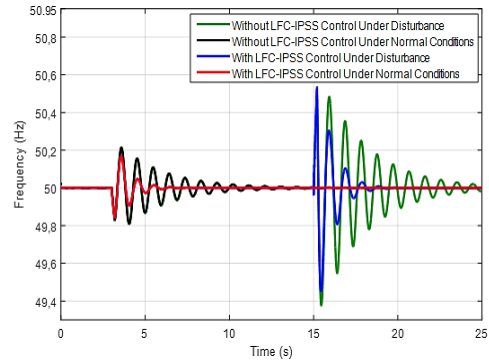


Fig. 12. Frequency Response of Generator

Likewise, grid security may involve also the analysis of each contingency of any disturbance occurring in the power system. Thus, a three-phase fault is investigated in this work. In fact, several studies gave great concern to this type of disturbance as the most severe one for transient stability problems. First, the fault occurs temporary on the load bus (bus 8) at time $t = 15$ s, and it is cleared at time $t = 15.2$ s.

The frequency oscillations are remarkably reduced and kept limited after the application of the designed system coordinating the optimized LFC with the IPSS. It reveals great damping of swings compared to the case where the performed controllers are not installed.

Actually, the performed IPSS provides an additional signal aiming essentially to dampen the generator torque oscillations. This control signal affords positive damping effect, while keeping the voltage level under its limit of stability. Fig. 13 reveals the voltage magnitude profile at bus 8 where the variable load is set.

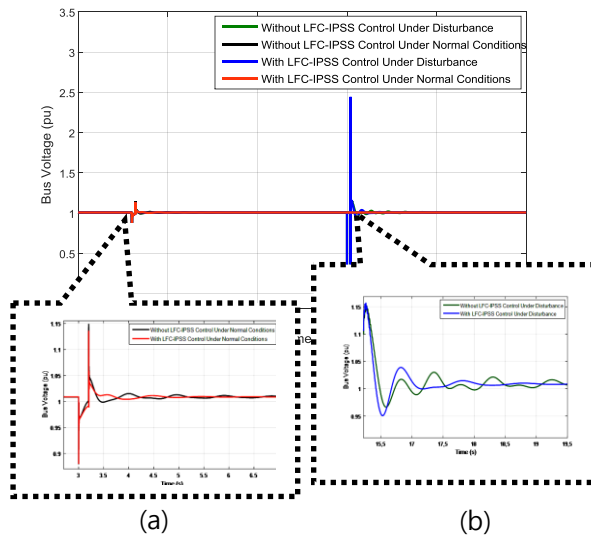


Fig. 13. Voltage Profile of Bus 8

Likewise, Fig. 13. (a) displays clearly a detailed zoom of the voltage oscillations of that bus at the moment of load demand rise at 5 under normal conditions. In fact, adding the IPSS to the current system delivers fast response with less number of swings and decreased amplitudes. Subsequently, Fig. 13. (b) shows great result only after installing the coordinated LFC-IPSS loops in the power system when subjected to a fault. It helps absolutely in keeping the voltage of the disturbed bus almost stable around the nominal value.

Furthermore, one other important variable that should be considered in the control process as to generator stability is basically related to its load angle. In fact, it demonstrates how close the machine is to the static stability limit. It increases proportionally with the active load: as well as the angle is amply large, the generator is close enough to the stability limit while keeping its synchronism.

Fig. 14 shows the load angle evolution of ‘Gen 2’. It’s remarkable that the load angle is retained between 20° to 30°. Consequently, it provides a great margin of stability whenever the power demand rises. The generator will be then able to outfit the load by increasing its load angle up to 90° maximally.

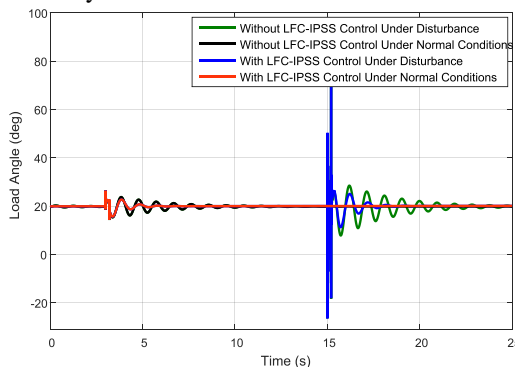


Fig. 14. Load Angle of Generator ‘Gen 2’
Equally, the control process involves

several operating parameters such as the electromagnetic torque and the rotor angle deviation especially to evaluate the dynamic system stability. The simulation results shown in Fig. 15 and Fig. 16 confirm the crucial role that the IPSS plays in damping the undesirable fluctuations in number and amplitude in order to enhance the system response to any sudden load variation. All the previous simulations prove that ensuring power system stability may require certainly powerful control tools including LFC and IPSS equipments.

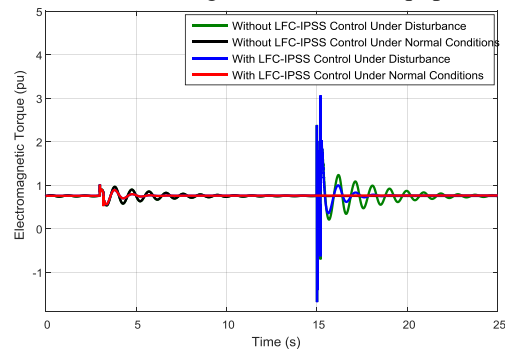


Fig. 15. Electromagnetic Torque of Generator ‘Gen 2’

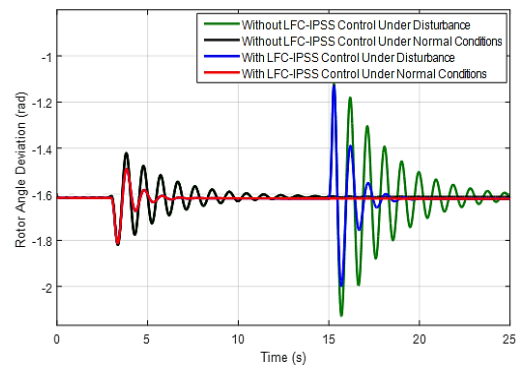


Fig. 16. Rotor Angle Deviation of Generator ‘Gen 2’

4.3. Evaluation of Wind Power Penetration

To analyze the impact of wind power generation on the dynamic behavior of the power system, different wind power penetration levels at 10 to 30 % are examined. In fact, two wind farms are installed in bus 9 and bus 7 just near to the designed power plants (Gen 3 and Gen 2, respectively). Each wind farm is connected locally to a 25 kV distribution system and consisted of DFIG wind turbines, rated 9 MW each. The system response is investigated first under normal conditions. Subsequently, in order to test the efficiency of the proposed controller in solving the system stability problem in presence of DFIG wind turbines, a three phase fault is created at the load bus (bus 8) at $t=15$ s and cleared at $t=15.2$ s. The frequency responses of generator ‘Gen 2’ for 10% and 20% of wind power penetration are presented in Fig. 17 and Fig. 18,

respectively.

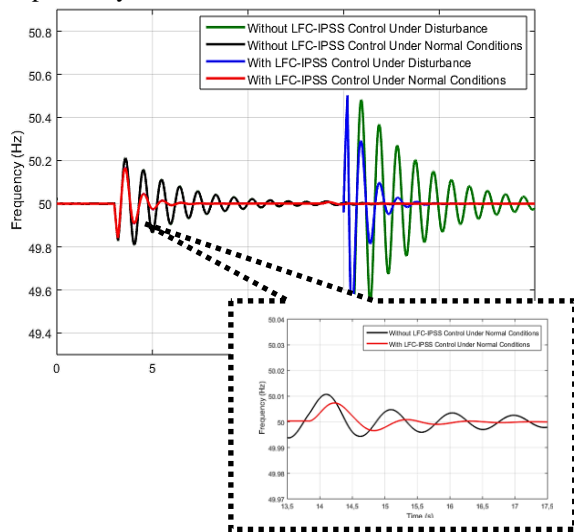


Fig. 17. Frequency Response of Generator 'Gen 2' with 10% wind penetration scenario

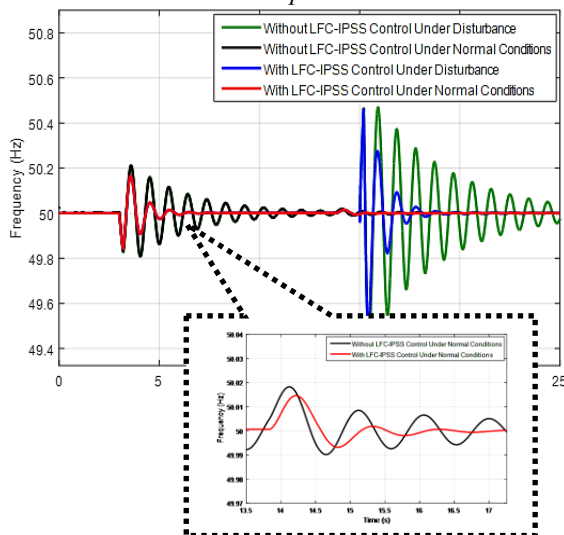


Fig. 18. Frequency Response of Generator 'Gen 2' with 20% wind penetration scenario

Obviously, the results are relatively similar. It is noticeable that on implementing coordinated LFC-IPSS process, when compared with the initial situation, the frequency of the machine under test achieves great response in terms of power oscillations especially when the wind farms generate the maximum of their power at 14 s as shown in detail in the zoomed in plot of the frequency responses of generator 'Gen 2'. The generator frequency oscillations demonstrate enhanced response too before, during and after the fault only in case where both of the performed LFC and IPSS regulators are involved in the grid's control system. Yet, when wind penetration increases beyond 30%, the frequency stability is

significantly degraded as shown in Fig. 19. The generator unit equipped with the proposed control scheme is unable to maintain ideally desirable frequency deviations. Thus, in order to keep stable operation of generators, the simulation study will be conducted mainly for 20% wind penetration into the test system. The installed DFIG wind turbines export in total 72 MW.

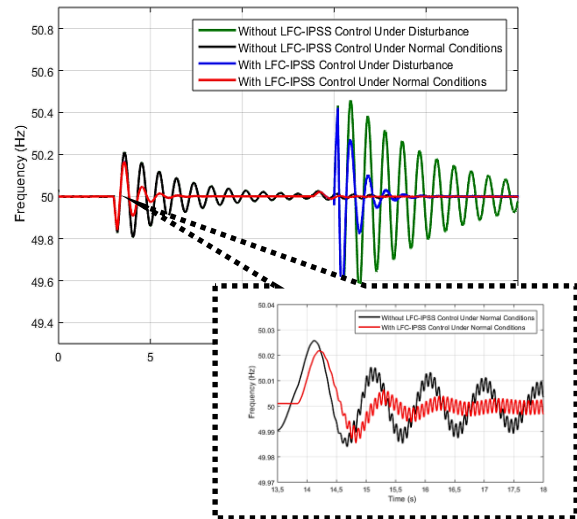


Fig. 19. Frequency Response of Generator 'Gen 2' with 30% wind penetration scenario

Practically, the generator torque evolution is one of the most challenging issues that should be controlled for system stability improvement purposes. In fact, it is clearly shown that injecting an intermittent power with rate of 72 MW to the power system is able enough to disturb the system waveforms. The more electrical power is generated, the more small fluctuations occur. Fig. 20 and Fig. 21 depict the electromagnetic torque and the load angle of generator 'Gen 2', respectively, before and after adding the proposed control scheme to the test system. It demonstrates considerable effect of these regulators in regaining approximately the nominal value reached in the initial case as well as maintaining the equilibrium of the system and damping the power oscillations. Additionally, applying a disturbance to the system may definitely result in change in frequency, load angle, machine's torque or voltage..., forcing the system to trip. Thus, only the wind turbine will operate until the fault is cleared. Therefore, the proposed controllers try to increase damping the maximum of the generated swings and regulate the waveforms at their set points.

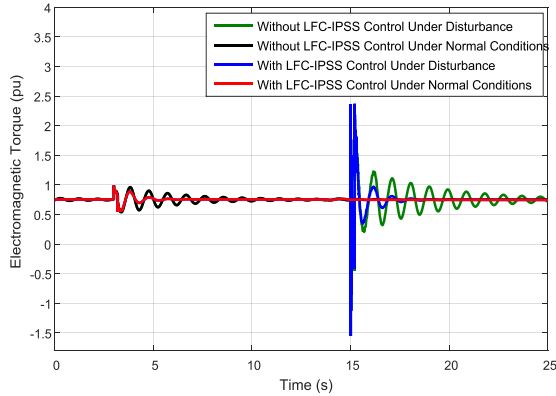


Fig. 20. Electromagnetic Torque of Generator 'Gen 2'

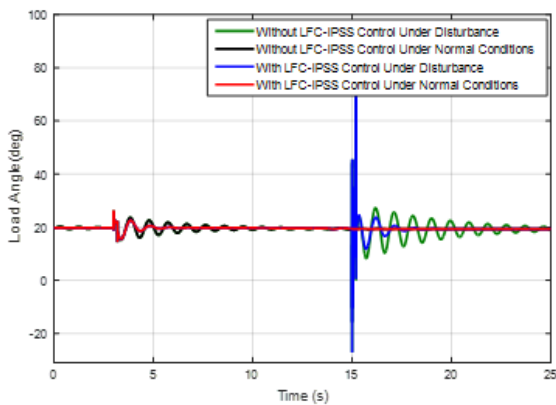


Fig. 21. Load Angle of Generator 'Gen 2'

The investigated wind farm is able enough to support the power system voltage during fault condition. In fact, DFIG wind turbines generate increasingly sufficient reactive power during the disturbance and decreases to its value after the fault clearance. Hence, in addition to DFIG support, coordinated LFC-IPSS process is also considered as shown in Fig. 22 which represents the voltage profile of the load bus under different operating conditions. Fig. 22. (a) proves that wind power incorporation may cause important voltage dip whenever involved with irrational rates. As well, Fig. 22. (b) which is a zoomed in plot of the bus voltage at the moment of fault reveals an improved oscillatory evolution roughly stable around the nominal value.

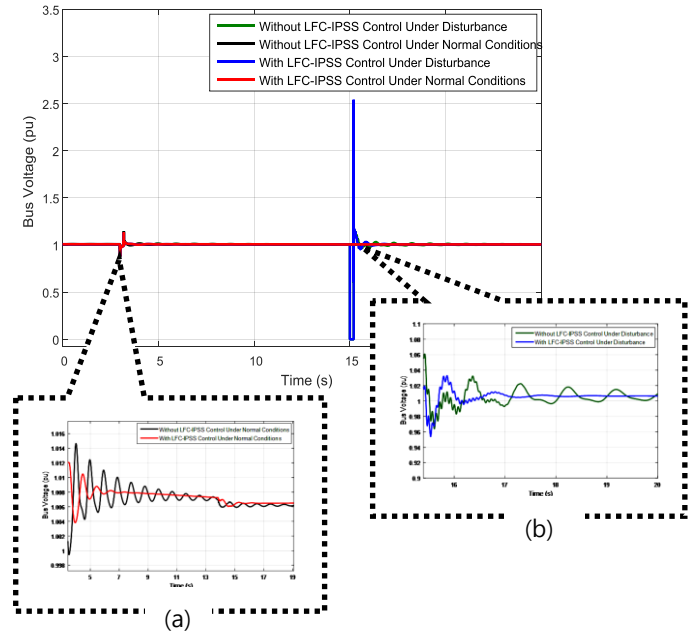


Fig. 22. Voltage Profile of Bus 8

5. Conclusion

The main contribution of this paper deals with designing and implementing a LFC based tuned-PI controller in coordination with an IPSS regulator under different operating conditions. This control scheme design is applied to the investigated model of the studied power system which shows effective response while enhancing its stability. In fact, robustness is critical in these control loops design since the loading conditions are unpredictably changing. An attempt is made first to PI controller which helps practically whenever tuned optimally in enhancing the dynamic performance of LFC in such interconnected power system. Actually, the use of H_∞ methodology for the tuning goal helps considerably in synthesizing PI controller in the frequency-domain. Typically, the controller design requirements such as speed of response, control bandwidth, disturbance rejection, and robust stability can be reached. However, in terms of speed of execution, it takes a significant amount of computer time. The comparison of different techniques proves that the H_∞ methodology provides the minimum values of the performance indices (ISE, IAE, and ITAE). Additionally, a great attention is given to system stability which is improved while integrating the designed IPSS loop. The tuning process is also investigated in the present work. In fact, the proposed IPSS settings show superior performances to the other settings in providing efficient damping of power system oscillations. Furthermore, the current study shows appreciable enhancements in the system response

in presence of the suggested control structure after being affected by DFIG wind turbines installation. The simulation results prove that optimized LFC and IPSS regulator is very effective and guarantees good dynamic performance under normal and fault conditions.

Nomenclature

| | |
|--------|--|
| LFC | Load Frequency Control |
| IPSS | Improved Power System Stabilizer |
| DFIG | Doubly Fed Induction Generator |
| ACE | Area Control Error |
| AGC | Automatic Generation Control |
| TG | Turbine Governor |
| PI | Proportional-Integral |
| PID | Proportional-Integral-Derivative |
| PSS | Power System Stabilizer |
| MB-PSS | Multi Band-Power System Stabilizer |
| ISE | Integral of the Square of the Error |
| IAE | Integral of the Absolute value of Error |
| ITAE | Integral of Time-weighted Absolute Error |

Appendix

System parameters [33]

Table 3. Synchronous generator parameters

| Parameters | Value |
|---|------------|
| Nominal power | |
| line-to-line voltage | 192 MVA |
| Nominal frequency | 13.8 KV |
| d-axis synchronous reactance, x_d | 50 Hz |
| d-axis transient reactance, X_d' | 1.305 pu |
| d-axis sub-transient reactance, X_d'' | 0.296 pu |
| q-axis synchronous reactance, X_q | 0.252 pu |
| q-axis sub-transient reactance, X_q' | 0.474 pu |
| Leakage reactance, X_l | 0.243 pu |
| d-axis transient short circuit time constant, T_d' | 0.18 pu |
| d-axis sub-transient short circuit time constant, T_d'' | 1.01 s |
| q-axis sub-transient open circuit time constant, T_{qo}'' | 0.053 s |
| Stator resistance, R_s | 0.1 s |
| Inertia coefficient, H | 0.00285 pu |
| | 3.7 pu |

Table 4. Hydraulic turbine and governor parameters

| Parameters | Value |
|-----------------------------|--------|
| Servo gain, K_a | 3.3 |
| Servo time constant, T_a | 0.07 s |
| Permanent droop, R_p | 0.05 |
| Water starting time, T_w | 2.67 s |
| Filter time constant, T_d | 0.01 |
| Proportional gain, K_p | 1.163 |
| Integral gain, K_i | 0.105 |
| Derivative gain, K_d | 0 |

Table 5. Excitation system parameters

| Parameters | Value |
|------------|-------|
|------------|-------|

| | |
|--|--------|
| Low-pass filter time constant, T_r | 0.02 s |
| voltage regulator gain, K_a | 300 |
| voltage regulator time constant, T_a | 0.001 |
| Exciter gain, K_e | s |
| Exciter time constant, T_e | 1 |
| Damping filter gain, K_f | 0 |
| Damping filter time constant, T_f | 0.001 |
| Transient gain reduction lag time constant, T_b | 0.1 s |
| Transient gain reduction lead time constant, T_c | 0 |

Table 6. DFIG parameters

| Parameters | Value |
|-------------------------------------|------------|
| Nominal power | 9 MW |
| Rated voltage | 575 V |
| Pair of poles | 3 |
| Rated frequency | 50 Hz |
| Stator resistance, R_s | 0.00706 pu |
| Rotor resistance, R_r | 0.005 pu |
| Stator leakage inductance, L_{ls} | 0.171 pu |
| Rotor leakage inductance, L_{lr} | 0.156 pu |
| Mutual inductance, L_m | 2.9 pu |
| Inertia constant, H | 5.04 s |
| Friction factor, F | 0.01 pu |

References

[1] K. Máslo, M. Kolcun, "Load-frequency control management in island operation", Electric Power Systems Research, vol. 114, pp 10-20, September 2014.

[2] J. Biswas, P. Bera, "Design of Rule-Based Load Frequency Controller for Multi-machine System", Industry Interactive Innovations in Science, Engineering and Technology, pp 47-57, July 2017

[3] H. Shayeghi, H.A. Shayanfar, and A. Jalili, "Load frequency control strategies: a state-of-the art survey for the researcher", Energy Conversion and Management, vol. 50, no. 2, pp 344-353, February 2009.

[4] D. Apostolopoulou, P.W. Sauer, and A.D. Dominguez-Garcia, "Automatic Generation Control and its Implementation in Real Time", 47th Hawaii International Conference on System Science, January 2014.

[5] M. Scherer, E. Iggland, A. Ritter, and G. Andersson, "Improved frequency bias factor sizing for non-interactive control", International Council on Large Electric Systems, pp C2-113, August 2012.

[6] H. Bevrani, T. Hiyama, "Intelligent Automatic Generation Control", pp 11-35, March 2017.

[7] H. Bevrani, "Robust Power System Frequency Control", pp 8-30, Springer, April 2014.

[8] X. Liu, X. Kong, K.Y. Lee, "Distributed model predictive control for load frequency control with dynamic fuzzy valve position modelling for hydro-thermal power system", IET Control Theory Applications., vol. 10, no. 14, pp. 1653-1664, September 2016.

[9] I. Nasiruddin, T.S. Bhatti and N. Hakimuddin, "Automatic Generation Control in an Interconnected Power System Incorporating Diverse Source Power Plants Using Bacteria Foraging Optimization Technique",

Electric Power Components and Systems, vol. 43, no 2, pp 189-199, December 2014.

[10] K. Tang, G.K.Venayagamoorthy, "Adaptive inter-area oscillation damping controller for multi-machine power systems", *Electric Power Systems Research*, vol. 134, pp 105-113, May 2016.

[11] S.K. Jain, A. Bhargava and R.K. Pal, "Three area power system load frequency control using fuzzy logic controller", *International Conference on Computer, Communication and Control*, pp 1-6, September 2015.

[12] K. Vrdoljak, N. Peric, and I. Petrovic, "Sliding mode based load frequency control in power systems", *Electric Power Systems Research*, vol.80, no. 5, pp. 514–527, May 2010.

[13] S.S. Dhillon, J.S. Lather, S. Marwaha, "Multi Area Load Frequency Control Using Particle Swarm Optimization and Fuzzy Rules", *Procedia Computer Science*, vol. 57, pp 460 – 472, August 2015.

[14] E. Rakhshani, J. Sadeh, "Application of Power System Stabilizer in a combined model of LFC and AVR loops to enhance system stability", *International Conference on Power System Technology*, October 2010.

[15] O. Abedinia, H. Shayanfar, B. Wyna, A. Ghasemi, "Design of Robust PSS to improve stability of composed LFC and AVR using ABC in deregulated environment", *Proceedings of the international conference on artificial intelligence*, July 2011.

[16] NY. Kouba, M. Mena, M. Hasni, M. Boudour, "A novel robust automatic generation control in interconnected multi-area power system based on bat inspired algorithm", *International Conference on Control, Engineering & Information Technology*, May 2015.

[17] I. Kamwa, R. Grondin, and G. Trudel, "IEEE PSS2B Versus PSS4B: The Limits of Performance of Modern Power System Stabilizers", *IEEE Transactions on Power Systems*, vol. 20, no. 2, pp 903 – 915, May 2005.

[18] G. Chen, Y. Sun, L. Cheng, J. Lina, W. Zhao, Ch. Lin, "A novel PSS-online re-tuning method", *Electric Power Systems Research*, vol. 91, pp 87-94, October 2012.

[19] Z. A. Obaid, L.M. Cipcigan, and M.T. Muhssin, "Power system oscillations and control: Classifications and PSSs' design methods: A review", *Renewable and Sustainable Energy Reviews*, vol. 79, pp 839-849, November 2017.

[20] S. M. Said, M.M. Aly and M. Abdel-Akher, "Capacity and Location Effects of Wind Turbine Energy Systems on Power Systems Stability", *International Journal on Power Engineering and Energy*, vol. 4, no. 1, January 2013.

[21] M. Zamanifar, B. Fani, M.E.H. Golshan, H.R. Karshenas, "Dynamic modeling and optimal control of DFIG wind energy systems using DFT and NSGA-II", *Electric Power Systems Research*, vol. 108, pp 50-58, March 2014.

[22] O. Barambones, J.A. Cortajarena, P. Alkorta and J.M. Gonzalez de Durana, "A real-time sliding mode control for a wind energy system based on a Doubly Fed Induction Generator", *Energies*, vol. 7, no. 10, pp 6412-6433, October 2014.

[23] L. L. Grigsby, "Power System Stability and Control", 3d Edition, Part 2, 8-1, April 2012.

[24] M.I. Alomoush, "Load frequency control and automatic generation control using fractional-order controllers", *Electrical Engineering*, vol. 91, no. 10, pp 357–368, March 2010.

[25] Ch. Huang, K. Zhang, X. Dai and Q. Zang, "Robust Load Frequency Controller Design Based on a New Strict Model", *Electric Power Components and Systems*, vol. 41, no. 11, pp 1075-1099, July 2013.

[26] P.S.R. Murty, "Power system analysis", 2nd Edition, Chapter 13, June 2017.

[27] P.Apkarian, P. Gahinet, and C. Buhr, "Multi-model, multi-objective tuning of fixed-structure controllers", *European Control Conference*, pp 856–861, July 2014.

[28] M.H. Marzaki, M. Tajjudin, M.H.F. Rahiman, R. Adnan, "Performance of FOPI with Error filter Based on Controllers Performance Criterion (ISE, IAE and ITAE)", *10th Asian Control Conference*, June 2015.

[29] J.M. Ramirez, R.E. Correa, and D.C. Hernández, "A strategy to simultaneously tune power system stabilizers", *International Journal of Electrical Power & Energy Systems*, vol. 43, no. 1, pp 818-829, December 2012.

[30] W. Yi, X. Lie, "Coordinated control of DFIG and FSIG-based wind farms under unbalanced grid conditions", *IEEE Transactions on Power Delivery*, vol. 25, no. 1, pp 367–377, January 2010.

[31] J. Yao, H. Li, Z. Chen, X. Xia, X. Chen, Q. Li, Y. Liao, "Enhanced Control of a DFIG Based Wind-Power Generation System With Series Grid-Side Converter Under Unbalanced Grid Voltage Conditions", *IEEE Transactions on Power Electronics*, vol. 28, no. 7, pp 3167 – 3181, September 2012.

[32] M.J. Zandzadeh, A. Vahedi, "Modeling and improvement of direct power control of DFIG under unbalanced grid voltage condition", *International Journal of Electrical Power & Energy Systems*, vol. 59, pp 58-65, July 2014.

[33] A. Delavari, I. Kamwa, P. Brunelle, "Simscape power systems benchmarks for education and research in power grid dynamics and control", *IEEE Canadian Conference on Electrical & Computer Engineering*, May 2018.